STRUCTURE AND FUNCTION

Rapid Evaluation of Right and Left Ventricular Function and Mass Using Real-Time True-FISP Cine MR Imaging Without Breath-Hold: Comparison with Segmented True-FISP Cine MR Imaging with Breath-Hold

Yoshiro Hori,[1,#] Naoaki Yamada,[1,*] Masahiro Higashi,[1] Nobuhiko Hirai,[1] and Satoshi Nakatani[2]

[1]Department of Radiology and Nuclear Medicine and [2]Cardiology Division of Medicine, National Cardiovascular Center, Suita, Osaka, Japan

ABSTRACT

Purpose. To evaluate the accuracy of cardiac function measured with real-time true fast imaging with steady-state precession (True-FISP) cine without breath-hold compared with those measured from segmented True-FISP cine with breath-hold. *Methods.* Eighteen consecutive patients and six healthy volunteers were enrolled in the study group. Both real-time multislice True-FISP cine imaging without breath-hold and single-slice segmented True-FISP cine imaging with multiple breath-holds were performed in short-axis imaging sections to encompass the entire ventricles. Vertical long-axis cine imaging using real-time True-FISP cine sequence without breath-hold was performed to evaluate heart motion during respiration in 13 subjects. Ventricular volume and mass were evaluated by four observers independently with manual tracing. *Results.* Real-time True-FISP cine quality was sufficient for contour detection in all 24 subjects. Cardiodynamic measurements based on real-time True-FISP cine correlated well with those based on segmented True-FISP cine [left ventricular (LV) end-diastolic volume: r = 0.98; LV end-systolic volume: r = 0.98; LV ejection fraction: r = 0.91; LV mass: r = 0.96; right ventricular (RV) end-diastolic volume: r = 0.89; RV end-systolic volume: r = 0.94; RV ejection fraction: r = 0.79]. Intra- and interobserver variability were sufficiently small in real-time True-FISP cine without breath-hold. Heart motion during respiration along the long axis of the left ventricle (2.2 mm to 3.7 mm) was much less than the slice interval (10 mm), confirming that misregistration of slice position during respiration was low. *Conclusion.* Real-time True-FISP cine without breath-hold has high reproducibility and is applicable to patients with severe cardiac dysfunction and/or arrhythmias.

[#]Present address: Department of Radiology, Niigata University School of Medicine, 1-757 Asahimachi-dori, Niigata City, 951-8510, Japan.

[*]Correspondence: N. Yamada, Department of Radiology and Nuclear Medicine, National Cardiovascular Center, 5-7-1, Fujishiro-dai, Suita, Osaka 565-8565, Japan; Fax: +81-6-6872-7486; E-mail: naoyamad@hsp.ncvc.go.jp.

Key Words: Magnetic resonance (MR); Cine study; Volume measurement; Heart; Real time; True FISP.

INTRODUCTION

Evaluation of accurate ventricular volume and function is important for management of myocardial disease. Traditionally, the gold standard for assessing the left ventricular (LV) volumes and ejection fraction (EF) was LV angiocardiography (Arvidsson, 1961; Chapman et al., 1958; Dodge et al., 1960; Sandler and Dodge, 1968). However, angiographic measurements depend upon a three-dimensional geometric model. In contrast to angiographic measurement, cine magnetic resonance (MR) imaging can acquire a three-dimensional data set and is independent of geometric assumption. Therefore, cine MR imaging is considered to be the most accurate clinical method for assessing ventricular volumes (Heusch et al., 1999; Debatin et al., 1992; Higgins, 1992; Rominger et al., 1999; Boxt et al., 1992; Sechtem et al., 1987; Pattynama et al., 1995).

With improved gradient performance, high signal at short time of repetition (TR), and high inherent blood/myocardial contrast, true fast imaging with steady-state precession (True-FISP) sequence, is now considered to be an excellent technique for rapid cine MR imaging of the heart (Carr et al., 2001; Lee et al., 2002; Barkhausen et al., 2001). However, in segmented True-FISP cine, repeated breath-holds of about ten seconds in duration are necessary to encompass the whole ventricle. In addition, patients with severe ventricular dysfunction or respiratory disease may not tolerate repeated breath-holds. In addition, arrhythmia degrades image quality.

True-FISP cine sequence can also be applied to real-time imaging, and when implemented at lower temporal and spatial resolution than single-slice segmented True-FISP cine sequence, real-time True-FISP cine is capable of acquiring multiple short-axis slices of the entire ventricle within 40 seconds.

The purpose of this study was to evaluate the accuracy of cardiac function measured from real-time True-FISP cine without breath-hold compared with those measured from segmented True-FISP cine with breath-hold.

MATERIALS AND METHODS

From April 10, 2001 through June 15, 2001, 18 patients who underwent MR imaging for evaluation of cardiac function (13 men and five women; mean age, 51 ± 14 years; age range, 18–72 years) and six healthy volunteers (all men; mean age, 33 ± 5 years; age range, 26–41 years) were enrolled in the study group. Main diagnosis of the patients were cardiomyopathy (n = 6: dilated cardiomyopathy, 4; hypertrophic cardiomyopathy, 1; arrhythmogenic right ventricular cardiomyopathy, 1); ischemic heart disease (n = 5: myocardial infarction, 4; angina pectoris 1); valvular heart disease (n = 3: aortic regurgitation, 1; mitral regurgitation, 1; pulmonary stenosis 1); pulmonary thromboembolism (n = 2); Fabry disease (n = 1); and myocarditis (n = 1). All the patients showed sinus rhythm during MR examination. The study was performed in accordance with the guidelines of the institutional review board. All volunteers and patients gave informed consent.

MR Imaging Technique

MR imaging was performed using a 1.5 T imager (Magnetom Quantum; Siemens Medical Systems, Erlangen, Germany) with high-performance gradients (maximum amplitude, 30 mT/m; maximum slew rate, 125 mT/m/msec).

After determining the vertical long axis of the left ventricle on the basis of transverse scout images, vertical long-axis cine imaging was performed for evaluation of heart motion during respiration by using real-time True-FISP cine sequence without breath-hold in nine patients and four volunteers. The subjects were told to breathe shallowly. Duration of the cine was 5 seconds to include the end-expiratory and end-inspiratory phase. Next, continuous short-axis cine images (8 mm slice thickness, 2 mm gaps) of the entire ventricle were obtained by using single-slice segmented True-FISP cine sequence (repetition time/echo time of 3.4 msec/1.7 msec, flip angle of 60°) with multiple breath-holds. Additionally, 12 to 14 short-axis cine images (8 mm slice thickness, 2 mm gaps) were obtained to encompass the entire ventricles by using real-time multislice True-FISP cine sequence (repetition time/echo time of 2.6 msec/1.3 msec, flip angle of 50°) without breath-hold. In both sequences, prospective electrocardiographic gating was performed by using the R wave as a trigger. The length of real-time scanning was adjusted to 1.3–1.5 times R–R interval at each slice. Because of the limitation of specific

absorption rate of electromagnetic wave in Japan, we used a flip angle of 50° in real-time True-FISP cine sequence, while a flip angle of 60° was used in segmented True-FISP cine sequence.

The real-time True-FISP cine sequence took 164 msec to acquire 63 k-space lines (63×2.6 msec). However, view-sharing techniques can generate intermediate temporal phase (Foo et al., 1995). In the real-time True-FISP cine used in this study, 28 of 63 lines were shared between the two temporally adjacent data sets (central seven lines were not shared), resulting in the effective temporal resolution of 91 msec [$(28 + 7) \times 2.6$ msec]. A segmented True-FISP cine sequence acquired 15 k-space lines per heartbeat, resulting in a temporal resolution of 51 msec (15×3.4 msec) without view sharing. The image data acquisition matrix of 63×128 for real-time True-FISP cine sequence and 120×256 for segmented True-FISP cine sequence were used with a rectangular field of view of 350 mm, which resulted in a pixel size of 4.17×2.73 mm for real-time True-FISP cine sequence and 1.82×1.37 mm for segmented True-FISP cine sequence.

Image Analysis

Ventricular volume and mass were analyzed by four observers independently with manual tracing of the epicardial and endocardial border using Siemens Argus software (Fig. 1). For the evaluation of interobserver variability, four observers were separated into two pairs at random in each subject, and one pair analyzed real-time True-FISP cine images and the other pair analyzed segmented True-FISP cine images. Each observer was unaware of the results by the other observers. For the evaluation of intraobserver variability, one observer reanalyzed ventricular volume and mass at least 2 weeks after initial evaluation. Because image data of one patient was broken, the evaluation of intraobserver variability was done on 23 subjects. In real-time True-FISP cine images, end-systolic and end-diastolic images were selected as the images with the smallest and the largest LV cavity, respectively. In segmented True-FISP cine images, end-diastolic images were selected as the first phase after triggering of the R wave, and end-systolic images were selected as the images with the smallest LV cavity. The basal slice was selected as the most basal slice in which myocardium was observed for LV, and as the most basal slice in which the cavity contracts and expands synchronously with LV by viewing the cine loops for RV. The papillary muscles were included in the ventricular chamber volume. End-diastolic and end-systolic volumes were calculated by summing the volumes of all short-axis slices (Simpson method). The myocardial mass was calculated from the difference of the volumes determined by the endocardial and epicardial contours of the left ventricle. The value 1.05 g/cm^3 was used as the density of the myocardium.

Evaluation of the heart motion during the respiration was done as follows (Fig. 2). First, in the vertical long-axis view of real-time True-FISP cine images, end-diastolic and end-systolic images at the end-inspiration and end-expiration were selected. Next, the apex and midpoint of the mitral valve in each image were selected (Fig. 2 A, A', B, B'). Then, displacement of the apex (AA') and the midpoint of the mitral valve (BB') were measured. Finally, length of projection on the long-axis direction (a,b) were measured.

Statistical Analysis

The mean value of the results by two observers in a pair was used for correlation analysis between real-time True-FISP cine and segmented True-FISP cine, and the correlation was evaluated by using linear regression and Bland-Altman analysis. Statistical significance of the differences between the results of the two sequences was assessed with the paired t-test. Differences with a P value less than 0.05 were considered to be significant. Both intra- and interobserver variability were calculated as the percentage of the absolute difference between the two measurements divided by the mean of the two measurements [(measurement 1 − measurement 2)/ mean of the two measurements].

RESULTS

Real-time True-FISP cine quality and contrast between blood and the endocardium were sufficient for contour detection in all 18 patients and six volunteers (Fig. 1). The total study time of imaging for real-time True-FISP cine was within 40 seconds, and it was significantly shorter than that for segmented True-FISP cine (approximately 15 min).

Real-time True-FISP cine correlated well with segmented True-FISP cine in left ventricular end-diastolic volume (LVEDV), left ventricular end-systolic volume (LVESV), and left ventricular ejection fraction (LVEF), r = 0.98, 0.98, and 0.91, respectively (Fig. 3A–F). Real-time True-FISP cine revealed a good correlation with segmented True-FISP cine in LV mass too (r = 0.96),
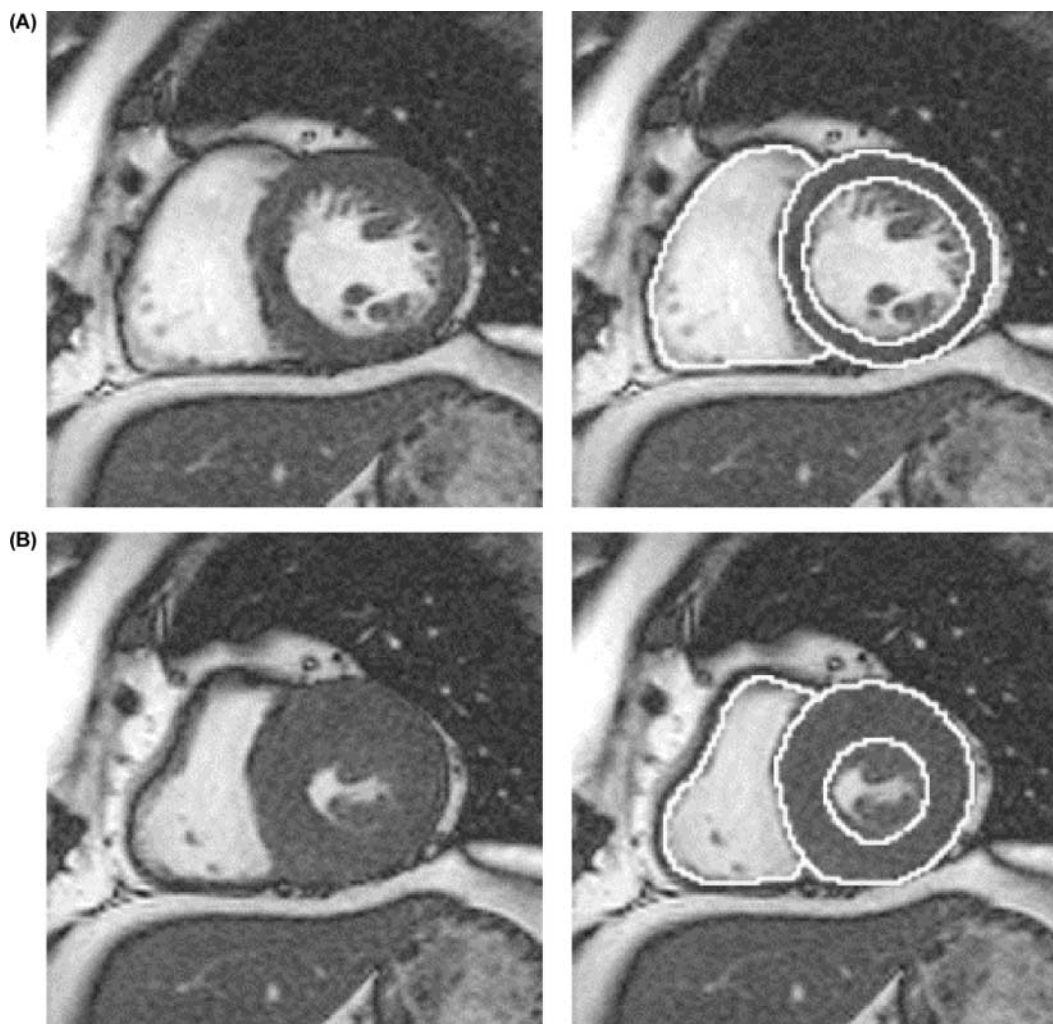
Figure 1. A 58-year-old woman with apical hypertrophic cardiomyopathy. Short-axis MR images obtained with segmented True-FISP cine (A: end-diastole; B: end-systole) and real-time True-FISP cine (C: end-diastole; D: end-systole). Right ventricular and left ventricular endocardial contours and left ventricular epicardial contours were traced manually. The papillary muscles were included in the ventricular cavity.

although LV mass was significantly underestimated in real-time True-FISP cine (Fig. 3G and H).

Correlations of right ventricular end-diastolic volume (RVEDV), right ventricular end-systolic volume (RVESV), and right ventricular ejection fraction (RVEF) between the two sequences were also good ($r = 0.89$, 0.94, 0.79, respectively), but these were not so good as the correlation of the LV measurements (Fig. 4A–F).

Table 1 summarizes the comparison of cardiodynamic measurements between real-time True-FISP cine and segmented True-FISP cine methods. As compared with segmented True-FISP cine, real-time True-FISP

cine significantly underestimated LV mass ($P < 0.01$). Furthermore, real-time True-FISP cine overestimated LVESV, and resulted in an underestimation of LVEF ($P < 0.05$).

Intra- and interobserver variability of real-time True-FISP cine and segmented True-FISP cine are summarized in Table 2. Interobserver variability was larger in real-time True-FISP cine than that in segmented True-FISP cine in all the measurements. Intraobserver variability was similar between real-time True-FISP cine and segmented True-FISP cine. Intra- and interobserver variabilities in real-time True-FISP cine in RV
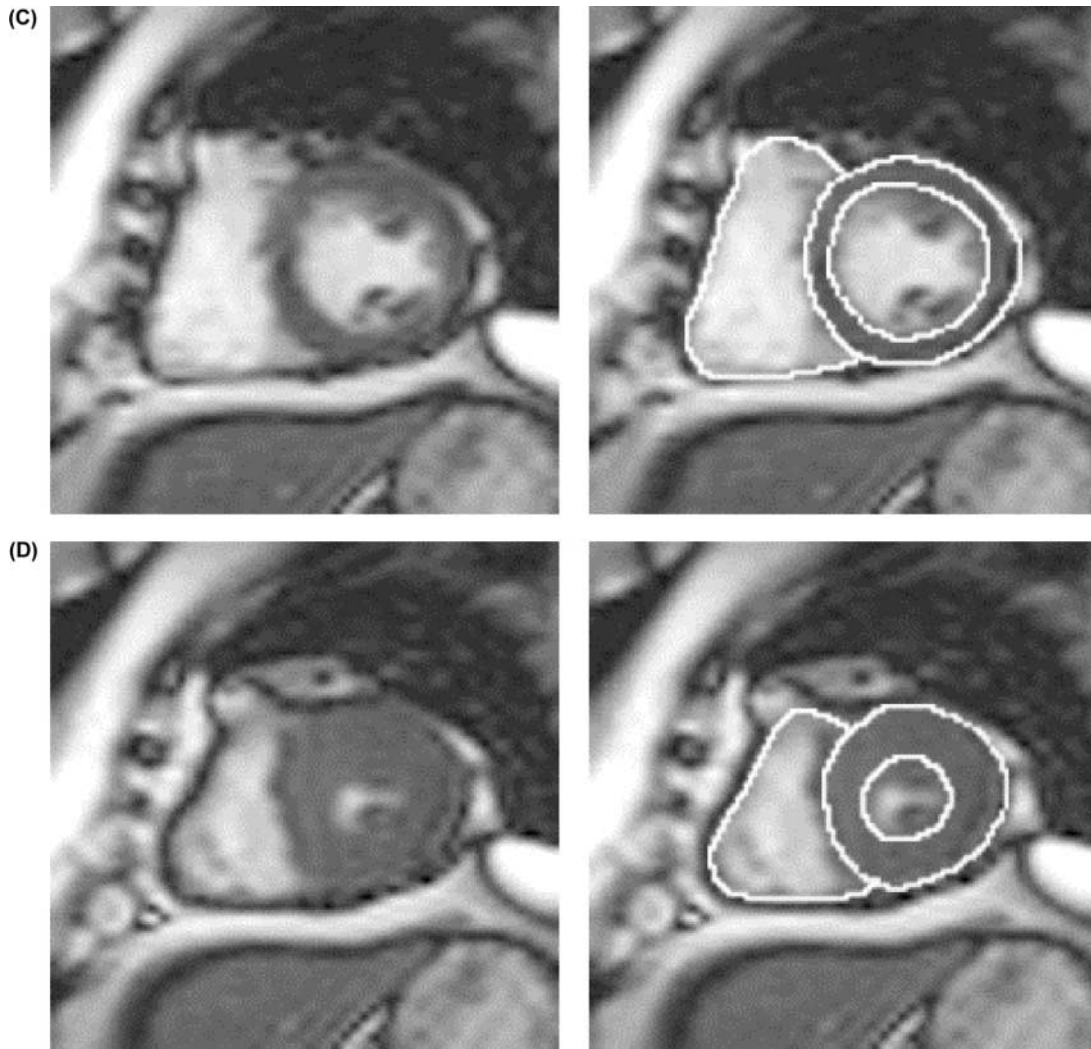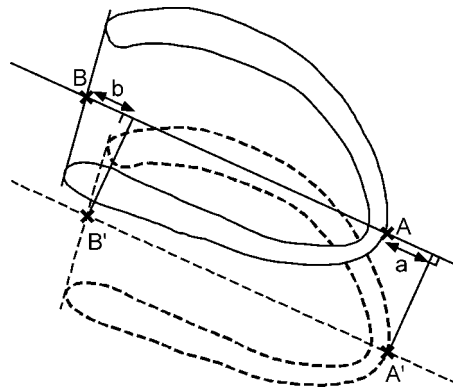
Figure 1. Continued.

Figure 2. Vertical long-axis view of the left ventricle at the end expiration (solid line) and end inspiration (dashed line). A = apex at the end expiration, A′ = apex at the end inspiration. B = midpoint of mitral valve at the end expiration, B′ = midpoint of mitral valve at the end inspiration. a = projection of AA′ on the long axis, b = projection of BB′ on the long axis.
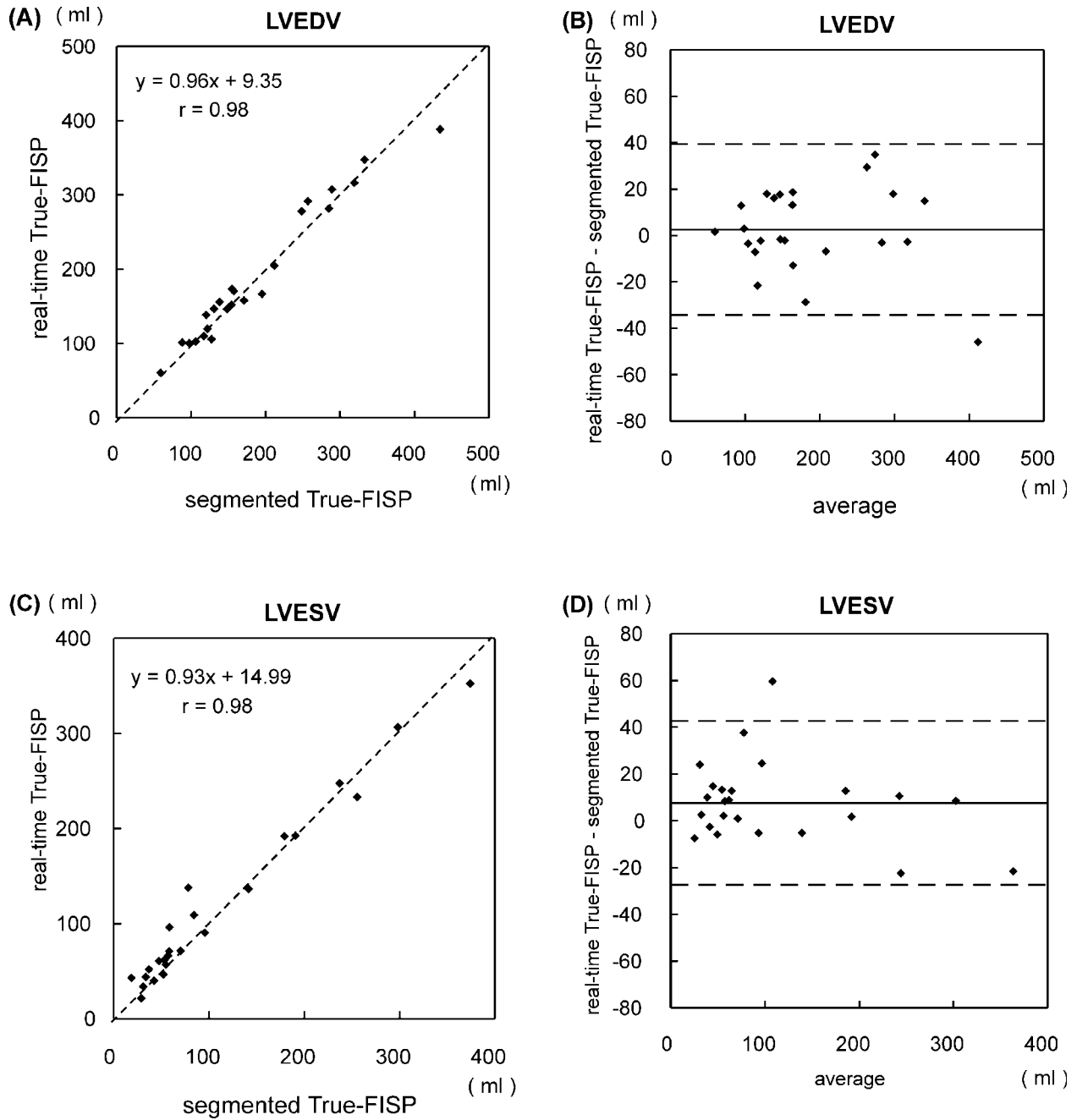
Figure 3. Scattered plots (A, C, E, G) and Bland-Altman plots (B, D, F, H) of LV measurements between real-time True-FISP and segmented True-FISP. In scattered plots, solid lines show regression line, dotted lines show the line of the identity. In Bland-Altman plots, the solid lines show mean difference, and dashed lines show 2 SD of the difference.

Rapid Evaluation of Right and Left Ventricular Function 445

(E) LVEF

$y = 0.77x + 7.49$
$r = 0.91$

(F) LVEF

(G) LV mass
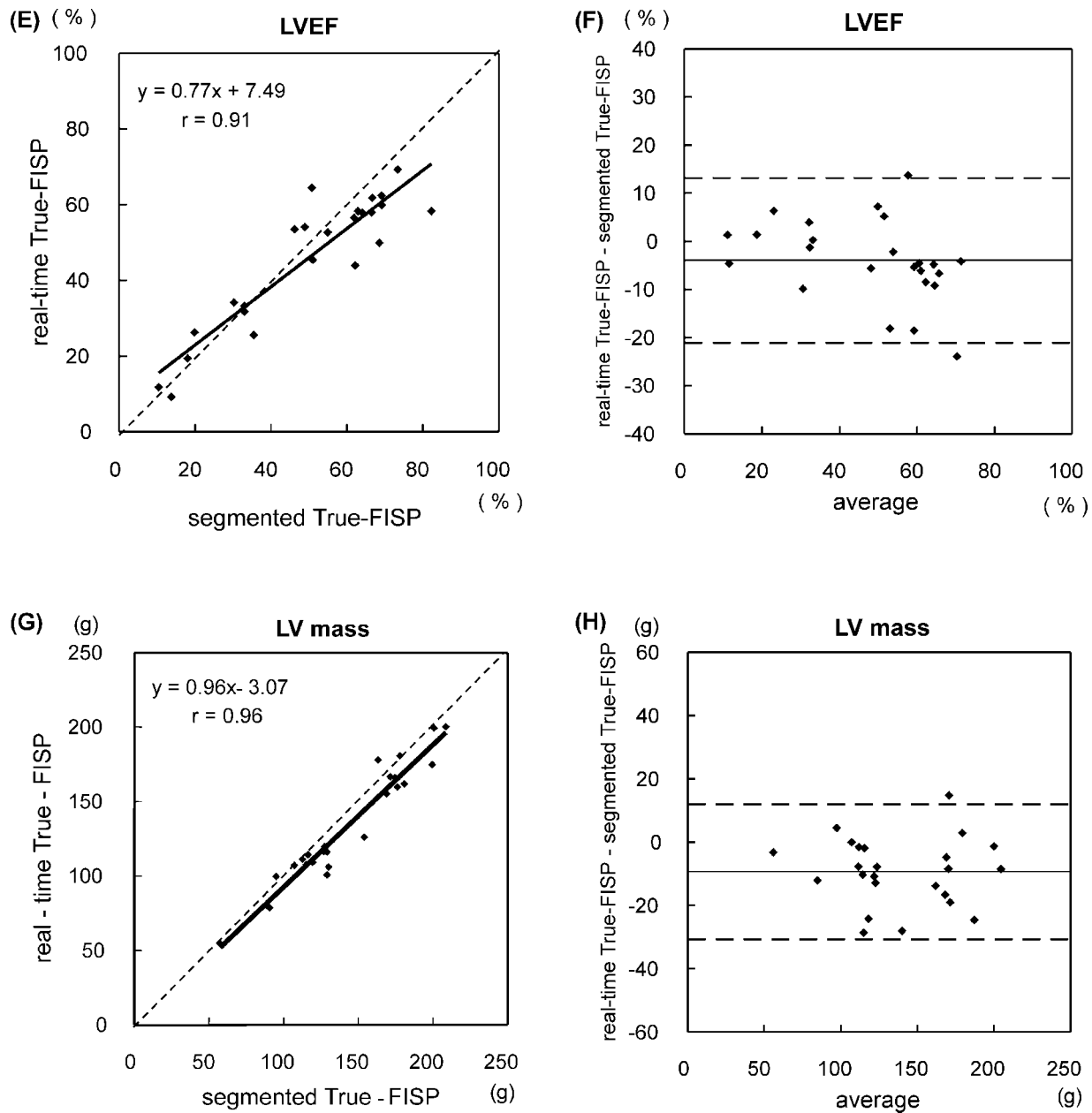
$y = 0.96x - 3.07$
$r = 0.96$

(H) LV mass

Figure 3. Continued.

measurements were larger than the corresponding variability in LV measurements. The variabilities in systolic volumes (LVESV and RVESV) were larger than the corresponding diastolic volumes (LVEDV and RVEDV). Absolute difference of the measurements, however, was similar between ESV and EDV.

Table 3 summarizes the heart motion during respiration. The mean displacement ranged from 4.6 mm to 6.0 mm, while the mean length of projection on long-axis direction ranged from 2.2 mm to 3.7 mm, which was much less than slice interval (10 mm).
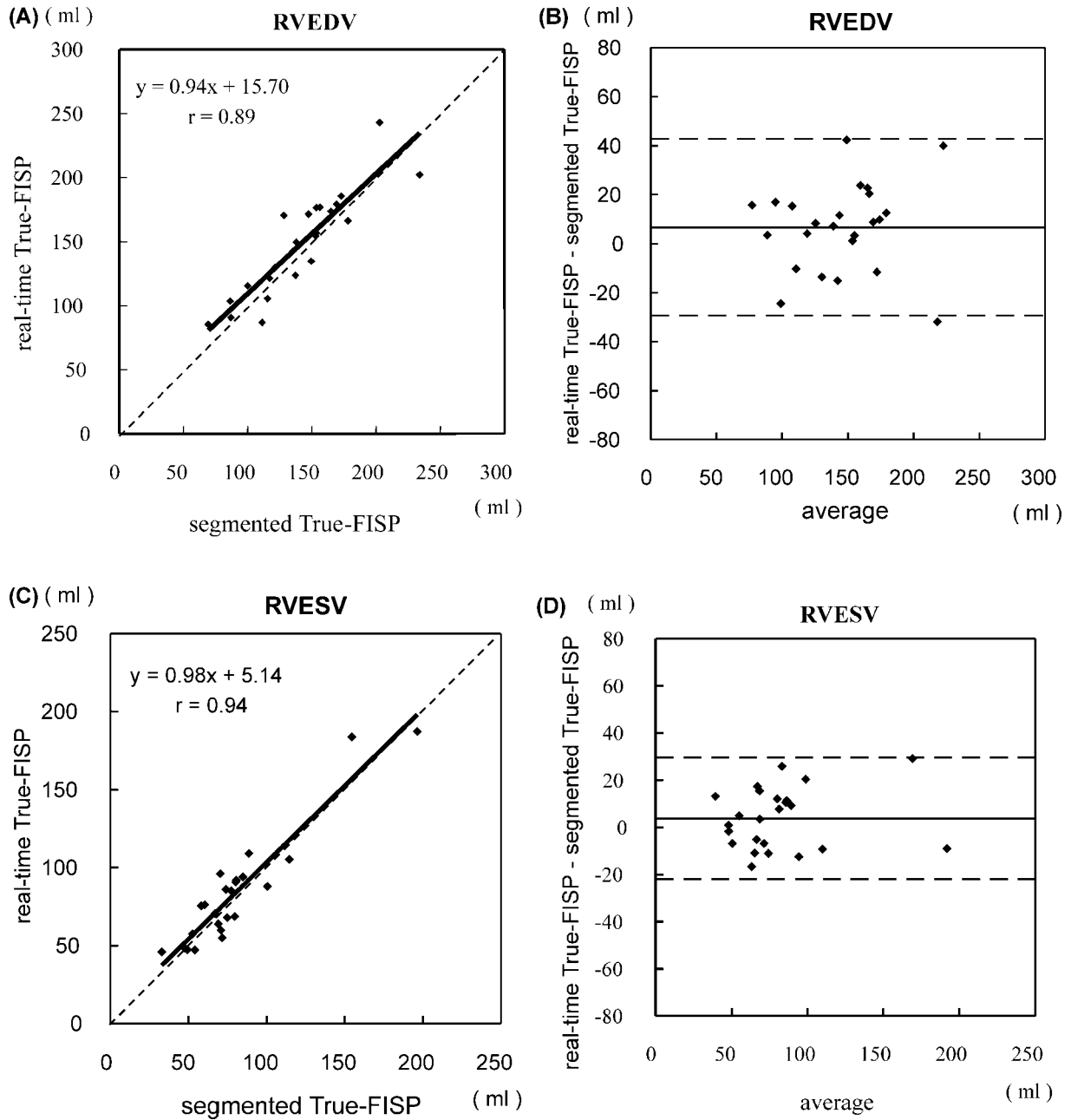
Figure 4. Scattered plots (A, C, E) and Bland-Altman plots (B, D, F) of RV measurements between real-time True-FISP and segmented True-FISP. In scattered plots, solid lines show regression line, dotted lines show the line of the identity. In Bland-Altman plots, the solid lines show mean difference, and dashed lines show 2 SD of the difference.
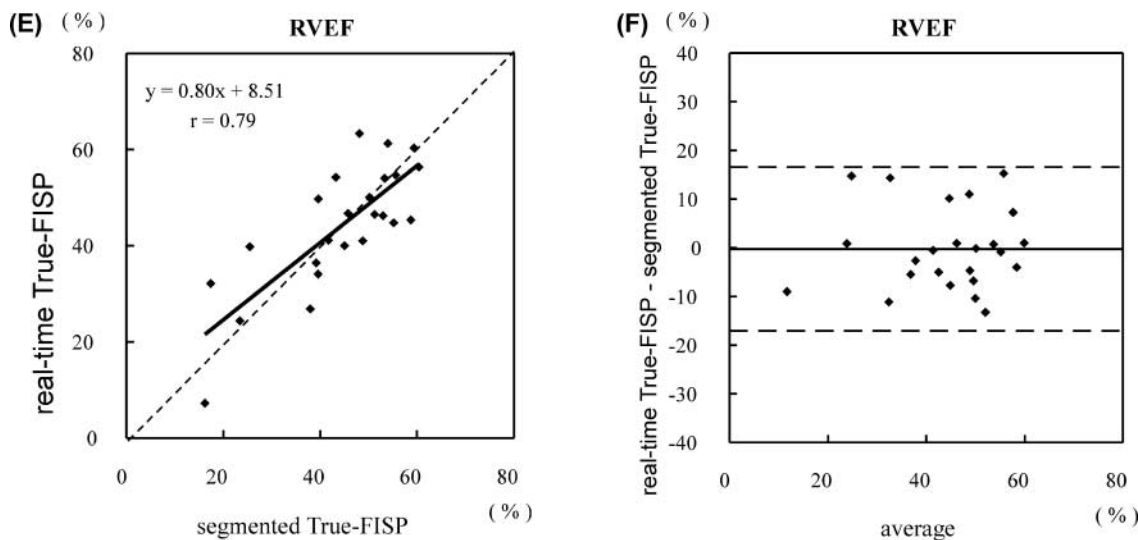
Figure 4. Continued.

DISCUSSION

Traditionally, spoiled gradient-echo fast low-angle shot (FLASH) MR imaging has been used for cardiac cine MR imaging. However, FLASH cine MR imaging relies on inflow enhancement to generate blood-myocardial contrast and, hence, is limited by low contrast-to-noise ratio at short TR and low-flow rates. A longer TR required for inflow enhancement in FLASH cine lengthens the acquisition time. Recently,

True-FISP cine sequence with segmentation of the k-space was developed and has been proven to be accurate for evaluation of ventricular volume and function. Segmented True-FISP cine MR imaging produces a higher blood-myocardial contrast and produces image quality superior to FLASH cine MR imaging (Carr et al., 2001; Lee et al., 2002). Due to the improved image quality, automatic delineation of the endocardial counter is more accurate when based on True-FISP cine images (Barkhausen et al., 2001).

Table 1. Comparison in cardiodynamic measurements between real-time True-FISP cine and segmented True-FISP cine.

	Real-time True-FISP	Segmented True-FISP	Absolute difference Mean	SD	r value
LVEDV (ml)	188 ± 91	186 ± 93	2.5	18.4	0.98
LVESV (ml)	115 ± 92	108 ± 97	7.6	17.5	0.98[a]
LVEF (%)	46 ± 17	50 ± 21	− 3.9	8.6	0.91[a]
LVmass (g)	134 ± 39	143 ± 39	− 9.3	10.7	0.96[b]
RVEDV (ml)	148 ± 39	141 ± 38	6.7	18.0	0.89
RVESV (ml)	83 ± 37	80 ± 35	3.8	12.9	0.94
RVEF (%)	44 ± 13	44 ± 13	− 0.2	8.4	0.79

LVEDV = left ventricular end-diastolic volume; LVESV = left ventricular end-systolic volume; LVEF = left ventricular ejection fraction; LV = left ventricular; RVEDV = right ventricular end-diastolic volume; RVESV = right ventricular end-systolic volume; RVEF = right ventricular ejection fraction; SD = standard deviation.
P values were determined with the paired t test.
[a] $P < 0.05$.
[b] $P < 0.01$.

Table 2. Intra and interobserver variability (mean difference ± standard deviation).

	Interobserver variability (n = 24)		Intraobserver variability (n = 23)	
	Real-time True-FISP	Segmented True-FISP	Real-time True-FISP	Segmented True-FISP
LVEDV	7.3 ± 5.1%	4.7 ± 4.2%	2.1 ± 2.1%	4.5 ± 4.5%
LVESV	14.0 ± 10.6%	8.9 ± 9.3%	6.0 ± 5.3%	9.3 ± 11.2%
LVEF	12.9 ± 9.8%	7.9 ± 8.8%	7.8 ± 9.5%	8.0 ± 7.0%
LV mass	14.6 ± 9.8%	8.8 ± 5.9%	7.7 ± 5.5%	4.8 ± 4.2%
RVEDV	13.9 ± 10.0%	8.8 ± 6.3%	6.9 ± 5.7%	5.1 ± 5.0%
RVESV	19.8 ± 15.1%	17.2 ± 10.9%	9.8 ± 8.7%	7.2 ± 4.0%
RVEF	24.5 ± 21.7%	20.9 ± 18.8%	10.1 ± 10.3%	8.2 ± 7.5%

LVEDV = left ventricular end-diastolic volume; LVESV = left ventricular end-systolic volume; LVEF = left ventricular ejection fraction; LV = left ventricular; RVEDV = right ventricular end-diastolic volume; RVESV = right ventricular end-systolic volume; RVEF = right ventricular ejection fraction.

However, repeated breath-hold of several heartbeats is needed for segmented True-FISP cine sequence. Therefore, in a patient with arrhythmia or inability to hold breath, the image quality may be degraded. Even in patients without arrhythmia who can hold breath, data acquisition under free breathing is easy and physiological. To solve these problems, we evaluated accuracy of real-time technique without breath-hold in comparison with breath-hold technique.

One of the problems using real-time True-FISP cine is the lower spatial resolution that can cause low accuracy of the cardiac border and poor separation of the ventricle from the atrium. Interobserver variability in cardiodynamic measurements obtained with real-time True-FISP cine was larger than that obtained with segmented True-FISP cine. Greater interobserver variability than that in previous reports (Boxt et al., 1992; Sechtem et al., 1987; Kaji et al., 2001; Sakuma et al., 1993; Pattynama et al., 1993; Semelka et al., 1990; Matheijssen et al., 1996) may be due to the fact that the evaluations in this study were performed by four observers as compared with the previous reports, in which evaluations were done by two observers. On the contrary, intraobserver variability in cardiodynamic measurements obtained with real-time True-FISP cine was similar to the results in previous reports (Butler et al., 1998; Sakuma et al., 1996) and the results obtained with segmented True-FISP cine in this study. In RV measurements, endocardial contour is more ambiguous than that of the LV due to the more prominent trabeculation and thin wall (Pattynama et al., 1995). So, intra- and interobserver variability in real-time True-FISP cine was larger in RV measurements than that in LV measurements.

Another problem in real-time True-FISP cine is a lower temporal resolution (data acquisition time 164 msec, and image reconstruction interval 91 msec in this study). The duration of isometric phase at end-systole was reported to be 70–80 msec (Spirito and Maron, 1988; Appleton et al., 1988), and duration of isovolumetric contraction at the end diastole is considered to be about 50 msec (Tojima et al., 1985).

Table 3. Heart motion during respiration.

	ED phase				ES phase			
	Apex		Midpoint of mitral valve		Apex		Midpoint of mitral valve	
	Displacement	Projection on long axis	Displacement	Projection on long axis	Displacement	Projection on long axis	Displacement	Projection on long axis
Mean	6.0 mm	3.7 mm	5.2 mm	2.8 mm	5.2 mm	2.2 mm	4.6 mm	2.2 mm
SD	4.1 mm	2.8 mm	4.2 mm	2.6 mm	4.2 mm	2.4 mm	2.5 mm	1.4 mm

ED = end-diastolic, ES = end-systolic, SD = standard deviation.

MARCEL DEKKER, INC. • 270 MADISON AVENUE • NEW YORK, NY 10016

Therefore, real-time True-FISP cine may not have hit the exact end systole and end diastole. Overestimation of LVESV, underestimation of LVEF, and underestimation of LV mass may be due to the lower temporal and spatial resolution, but absolute differences of the quantities were not large (Table 1) and were in allowable range.

The greatest concern in data acquisition without breath-hold is displacement of the heart under free breathing that may cause error in the measurements. Schalla et al. obtained good correlation between breath-hold real-time cine and segmented cine: 0.99 for LVEDV, 0.95 for LVESV, 0.96 for LVEF, and 0.81 for LV mass (Schalla et al., 2001). Kaji et al. acquired data of real-time cine under free breathing for at least 8 heartbeats at each slice and selected cardiac cycle at end expiration, and obtained correlation with a segmented gradient echo 0.944–0.986 for LVEDV, 0.944–0.994 for LVESV, 0.892–0.982 for LVEF, and 0.963 for LV mass (Kaji et al., 2001). On the contrary, imaging of real-time cine of this study was performed without breath-hold and in a short time (1.3 to 1.5 heartbeat at each slice, total imaging time less than 40 seconds). In the results, nevertheless, correlation between real-time cine and segmented cine in our study was as high as the previous reports. We showed that heart motion along the long-axis direction is much less than slice interval, and therefore the misregistration error under free breathing could be small when a patient breathed calmly. If an arrhythmia does not occur during data acquisition, our method gives acceptable cardiodynamic measurements.

Intra- and interobserver variability in real-time True-FISP cine was similar to or less than the other modalities. In an angiographic study, Cohn et al. reported that the average interobserver difference in LV volume and EF was 8.5–12% when the same ventriculogram was measured by different observers (Cohn et al., 1974). In a two-dimensional echocardiographic study by Starling et al., the average interobserver differences were 26% for LVEDV, 22% for LVESV, and 8.1% for LVEF, and the average intraobserver differences were 10% for LVEDV, 12.4% for LVESV, and 5.1% for LVEF (Starling et al., 1981). Therefore, our results of intra- and interobserver variability are within an allowable range. Quantitative gated single photon emission computed tomography (SPECT) (QGS), performed under free breathing, has become widely used for computation of ventricular volumes and EF (Germano et al., 1995), and this automated method has high reproducibility. But QGS is confounded by the presence of large perfusion defects or extracardiac background activity (Vallejo et al., 2000).

In summary, cardiodynamic measurements obtained with real-time True-FISP cine under free breathing correlated well with segmented True-FISP cine. In the future, further reduction of TR or the use of recently developed parallel imaging techniques such as SENSE or SMASH (Pruessmann et al., 1999; Sodickson and Manning, 1997; Jakob et al., 1999) can improve temporal resolution. Real-time cine MR imaging is promising and essential in the evaluation of cardiodynamics.

REFERENCES

Appleton, C. P., Hatle, L. K., Popp, R. L. (1988). Relation of transmitral flow velocity patterns to left ventricular diastolic function: new insights from a combined hemodynamic and Doppler echocardiographic study. *J. Am. Coll. Cardiol.* 12:426–440.

Arvidsson, H. (1961). Angiocardiographic determination of left ventricular volume. *Acta Radiol.* 56:321–339.

Barkhausen, J., Ruehm, S. G., Goyen, M., Buck, T., Laub, G., Debatin, J. F. (2001). MR evaluation of ventricular function: true fast imaging with steady-state precession versus fast low-angle shot cine MR imaging: feasibility study. *Radiology* 219:264–269.

Boxt, L. M., Katz, J., Kolb, T., Czegledy, F. P., Barst, R. J. (1992). Direct quantitation of right and left ventricular volumes with nuclear magnetic resonance imaging in patients with primary pulmonary hypertension. *J. Am. Coll. Cardiol.* 19:1508–1515.

Butler, S. P., Mckay, E., Paszkowski, A. L., Quinn, R. J., Shnier, R. C., Donovan, J. T. (1998). Reproducibility study of left ventricular measurements with breath-hold cine MRI using a semiautomated volumetric image analysis program. *J. Magn. Reson. Imaging* 8:467–472.

Carr, J. C., Simonetti, O., Bundy, J., Li, D., Pereles, S., Finn, J. P. (2001). Cine MR angiography of the heart with segmented true fast imaging with steady-state precession. *Radiology* 219:828–834.

Chapman, C. B., Baker, O., Reynolds, J., Bonte, F. J. (1958). Use of biplane cinefluorography for measurement of ventricular volume. *Circulation* 18:1105–1117.

Cohn, P. F., Levine, J. A., Bergeron, G. A., Gorlin, R. (1974). Reproducibility of the angiographic left ventricular ejection fraction in patients with coronary artery disease. *Am. Heart J.* 88:713–720.

Debatin, J. F., Nadel, S. N., Paolini, J. F., et al. (1992). Cardiac ejection fraction: phantom study comparing cine MR imaging, radionuclide blood pool imaging, and ventriculography. *J. Magn. Reson. Imaging* 2:135–142.

Dodge, H. T., Sandler, H., Ballew, D. W., Lord, J. D. (1960). The use of biplane angiography for the measurement of left ventricular volume in man. *Am. Heart J.* 60:762–776.

Foo, T. K., Bernstein, M. A., Aisen, A. M., Hernandez, R. J., Collick, B. D., Bernstein, T. (1995). Improved ejection

fraction and flow velocity estimates with use of view sharing and uniform repetition time excitation with fast cardiac techniques. *Radiology* 195:471–478.

Germano, G., Kiat, H., Kavanagh, P. D., et al. (1995). Automatic quantification of ejection fraction from gated myocardial perfusion SPECT. *J. Nucl. Med.* 36:2138–2147.

Heusch, A., Koch, J. A., Krogmann, O. N., Korbmacher, B., Bourgeois, M. (1999). Volumetric analysis of the right and left ventricle in a porcine heart model: comparison of three-dimensional echocardiography, magnetic resonance imaging and angiocardiography. *Eur. J. Ultrasound* 9:245–255.

Higgins, C. B. (1992). Which standard has the gold? *J. Am. Coll. Cardiol.* 19:1608–1609.

Jakob, P. M., Griswold, M. A., Edelman, R. R., Manning, W. J., Sodickson, D. K. (1999). Accelerated cardiac imaging using the SMASH technique. *J. Cardiovasc. Magn. Reson.* 1:153–157.

Kaji, S., Yang, P. C., Kerr, A. B., et al. (2001). Rapid evaluation of left ventricular volume and mass without breath-holding using real-time interactive cardiac magnetic resonance imaging system. *J. Am. Coll. Cardiol.* 38:527–533.

Lee, V. S., Resnick, D., Bundy, J. M., Simonetti, O. P., Lee, P., Weinreb, J. C. (2002). Cardiac function: MR evaluation in one breath hold with real-time true fast imaging with steady-state precession. *Radiology* 222:835–842.

Matheijssen, N. A., Baur, L. H., Reiber, J. H., et al. (1996). Assessment of left ventricular volume and mass by cine magnetic resonance imaging in patients with anterior myocardial infarction intra-observer and inter-observer variability on contour detection. *Int. J. Card Imaging* 12:11–19.

Pattynama, P. M., Lamb, H. J., van der Velde, E. A., van der Wall, E. E., de Roos, A. (1993). Left ventricular measurements with cine and spin-echo MR imaging: a study of reproducibility with variance component analysis. *Radiology* 187:261–268.

Pattynama, P. M., Lamb, H. J., van der Velde, E. A., Van der Geest, R. J., van der Wall, E. E., de Roos, A. (1995). Reproducibility of MRI-derived measurements of right ventricular volumes and myocardial mass. *Magn. Reson. Imaging* 13:53–63.

Pruessmann, K. P., Weiger, M., Scheidegger, M. B., Boesiger, P. (1999). SENSE: sensitivity encoding for fast MRI. *Magn. Reson. Med.* 42:952–962.

Rominger, M. B., Bachmann, G. F., Pabst, W., Rau, W. S. (1999). Right ventricular volumes and ejection fraction with fast cine MR imaging in breath-hold technique: applicability, normal values from 52 volunteers, and evaluation of 325 adult cardiac patients. *J. Magn. Reson. Imaging* 10:908–918.

Sakuma, H., Fujita, N., Foo, T. K., et al. (1993). Evaluation of left ventricular volume and mass with breath-hold cine MR imaging. *Radiology* 188:377–380.

Sakuma, H., Globits, S., Bourne, M., Shimakawa, A., Foo, T., Higgins, C. (1996). Improved reproducibility in measuring LV volumes and mass using multicoil breath-hold cine MR imaging. *J. Magn. Reson. Imaging* 6:124–127.

Sandler, H., Dodge, H. T. (1968). The use of single plane angiocardiograms for the calculation of left ventricular volume in man. *Am. Heart J.* 75:325–334.

Schalla, S., Nagel, E., Lehmkuhl, H., et al. (2001). Comparison of magnetic resonance real-time imaging of left ventricular function with conventional magnetic resonance imaging and echocardiography. *Am. J. Cardiol.* 87:95–99.

Sechtem, U., Pflugfelder, P. W., Gould, R. G., Cassidy, M. M., Higgins, C. B. (1987). Measurement of right and left ventricular volumes in healthy individuals with cine MR imaging. *Radiology* 163:697–702.

Semelka, R. C., Tomei, E., Wagner, S., et al. (1990). Interstudy reproducibility of dimensional and functional measurements between cine magnetic resonance studies in the morphologically abnormal left ventricle. *Am. Heart J.* 119:1367–1373.

Sodickson, D. K., Manning, W. J. (1997). Simultaneous acquisition of spatial harmonics (SMASH): ultra-fast imaging with radiofrequency coil arrays. *Magn. Reson. Med.* 38:591–603.

Spirito, P., Maron, B. J. (1988). Influence of aging on Doppler echocardiographic indices of left ventricular diastolic function. *Br. Heart J.* 59:672–679.

Starling, M. R., Crawford, M. H., Sorensen, S. G., Levi, B., Richards, K. L., O'Rourke, R. A. (1981). Comparative accuracy of apical biplane cross-sectional echocardiography and gated equilibrium radionuclide angiography for estimating left ventricular size and performance. *Circulation* 63:1075–1084.

Tojima, H., Harumi, K., Ishikawa, K., et al. (1985). Clinical cardiology vol.1: fundamentals for the cardiovascular clinic: Chugai Igaku.

Vallejo, E., Dione, D. P., Bruni, W. L., et al. (2000). Reproducibility and accuracy of gated SPECT for determination of left ventricular volumes and ejection fraction: experimental validation using MRI. *J. Nucl. Med.* 41:874–882.